Intratumoral Metabolic Heterogeneity of Cervical Cancer

Elizabeth A. Kidd[1] and Perry W. Grigsby[1,2,3,4]

Abstract

Purpose: Previous research has shown that the intertumoral maximum standardized uptake value (SUV_{Max}) of F-18 fluorodeoxyglucose (FDG)–positron emission tomography (PET) for cervical cancer predicts disease outcome. The purpose of this study was to evaluate the pretreatment intratumoral metabolic heterogeneity of FDG.

Experimental Design: This is a prospective cohort study of 72 patients with International Federation of Gynecology and Obstetrics stages Ib1 to IVa cervical cancer treated with chemoradiation. Three-dimensional FDG-PET threshold tumor volumes were calculated using image segmentation and an adaptive thresholding method for the primary cervix tumor from the pretreatment FDG-PET/computerized tomography. Intratumor heterogeneity was obtained for each patient's cervical tumor by taking the derivative (dV/dT) of the volume-threshold function from 40% to 80%. The association between intratumoral heterogeneity and tumor-specific factors and patient outcomes were determined.

Results: The mean cervix tumor SUV_{Max} was 12.4 (range, 3.0-38.4). The mean differential tumor heterogeneity was -1.074 (range, -0.107 to -5.623). There was no association between dV/dT and SUV_{Max} ($R^2 = 0.069$), but there was a relationship with dV/dT and tumor volume ($R^2 = 0.881$). There was no correlation of dV/dT with tumor histology ($P = 0.4905$). Heterogeneity was significantly associated with the risk of lymph node metastasis at diagnosis ($P = 0.0009$), tumor response to radiation as evaluated by FDG-PET obtained 3 months after completing treatment ($P = 0.0207$), risk of pelvic recurrence ($P = 0.0017$), and progression-free survival ($P = 0.03$).

Conclusions: Cervical intratumoral FDG metabolic heterogeneity on the pretreatment FDG-PET predicts risk of lymph node involvement at diagnosis, response to therapy, and risk of pelvic recurrence.

It is understood that, on a microscopic level, tumors are heterogeneous (1–3). Evaluation of tumor microenvironments has shown heterogeneity relating to variation in tumor responsiveness to treatment (4, 5), degree of vascularity (6, 7), hypoxia (1, 7, 8), proliferation rates (7), energy metabolites, and gene expression (9–11). Although tumor heterogeneity has been shown within these tumor microenvironments, intratumoral heterogeneity across the entire volume of primary tumors in humans has not been quantified or analyzed for its association with outcome measures. F-18 fluorodeoxyglucose (FDG)–positron emission tomography (PET) imaging allows intratumoral heterogeneity to be assessed using objective criteria.

Cervical cancer is an example of a tumor that shows heterogeneity relating to hypoxia, variation in response to treatment, risk of metastatic spread, and gene expression (4, 5, 10, 12–15). Additionally, the response of the primary cervical cancer to treatment has been shown to be a much more complex issue than simply relating outcome to clinical stage, tumor volume, or tumor hypoxia. Specifically, our previous research has shown that the primary cervix tumor maximal standardized uptake value (SUV_{Max}) on FDG-PET is predictive of disease prognosis and outcome irrespective of tumor stage or tumor volume (16, 17). We have observed that this primary cervix tumor glucose metabolism (SUV signal intensity) from the FDG-PET image can vary greatly across the volume of individual cervical tumors (18).

Our objective with this study was to quantitatively measure cervical intratumoral FDG metabolic heterogeneity, as observed on the pretreatment FDG-PET/computerized tomography (CT) and explore the relationship of this heterogeneity to treatment outcome. By analyzing the variation in glucose metabolism over the entire volume of the tumor, a differential of metabolic heterogeneity (H) was obtained, thus providing a single numerical value reflecting tumor heterogeneity. Heterogeneity was analyzed for its association with tumor and outcome measures, including tumor histology, risk of lymph node involvement at diagnosis, response to treatment, and recurrence risk.

Authors' Affiliations: [1]Department of Radiation Oncology, [2]Division of Nuclear Medicine, Mallinckrodt Institute of Radiology, [3]Department of Obstetrics and Gynecology, and [4]the Alvin J. Siteman Cancer Center, Washington University Medical Center, St. Louis, Missouri

Received 1/3/08; revised 4/28/08; accepted 5/4/08.

The costs of publication of this article were defrayed in part by the payment of page charges. This article must therefore be hereby marked *advertisement* in accordance with 18 U.S.C. Section 1734 solely to indicate this fact.

Requests for reprints: Perry W. Grigsby, Washington University School of Medicine, Department of Radiation Oncology, Campus Box 8224, Mallinckrodt Institute of Radiology, 4921 Parkview Place, CAM Lower Level, St. Louis, MO 63110. Phone: 314-362-8502; Fax: 314-747-9557; E-mail: pgrigsby@wustl.edu.

doi:10.1158/1078-0432.CCR-07-5252

Table 1. Patient and tumor characteristics

Baseline characteristics	All patients
Age at diagnosis, y	Mean, 51.4; range, 24-83
Stage	
Ib1	7
Ib2	12
IIa	2
IIb	38
IIIa	2
IIIb	10
IVa	1
Histology	
Squamous	63
Adenocarcinoma	7
Clear cell	2
Lymph node status at diagnosis	
None	37
Pelvic lymph nodes	23
Para-aortic lymph nodes	8
Supraclavicular lymph nodes	4

Materials and Methods

Patients. This is a prospective cohort study of 72 patients with International Federation of Gynecology and Obstetrics stage Ib to IVa cervical cancer treated at Washington University in St. Louis from April 2005 to July 2007. The Washington University Human Research Protection Office approved this research. All patients underwent a pretreatment whole-body FDG-PET/CT. Patients were staged clinically according to International Federation of Gynecology and Obstetrics staging, with the distribution as follows: 7 patients with stage Ib1, 12 with stage Ib2, 2 with stage IIa, 38 with stage IIb, 2 with stage IIIa, 10 with stage IIIb, and 1 with stage IVa. The pathologic diagnosis of all tumors was determined by Washington University pathologists, with histology as follows: squamous cell carcinoma in 63, adenocarcinoma in 7, and clear cell carcinoma in 2. Patient age ranged from 24 to 83 y (mean, 51.4 y). Lymph node metastasis at diagnosis, as determined by FDG-PET/CT, was present in 35 patients (Table 1).

Treatment. All patients were treated with concurrent chemotherapy and radiation. FDG-PET/CT imaging was used to define the extent of the metabolically active disease for radiation treatment planning. The radiation was based on standard treatment practices of external IMRT irradiation and HDR brachytherapy for cervical cancer at Washington University in St. Louis (19). Chemotherapy consisted of cisplatin (40 mg/m^2 weekly for six cycles).

FDG-PET/CT technique and image analysis. FDG-PET/CT was done in all patients with a hybrid PET/CT scanner (Biograph LSO 2, Siemens Medical Solutions). The CT portion of the study was done without the administration of i.v. contrast. CT images (5-mm slices) were obtained from the base of skull through the proximal thighs at 130 kVp and 110 effective mA. PET images were obtained over the same anatomic extent beginning 42 to 120 min (median, 65 min) after the administration of 15 to 20 mCi FDG, with imaging times of 2 to 4 min/bed position, depending on patient weight. Serum glucose levels ranged from 75 to 187 (median, 105). Urinary tract activity was minimized by the placement of a Foley catheter before injection of FDG and by administration of furosemide and i.v. fluids after injection of FDG in most patients. PET images were scatter corrected and reconstructed using ordered-subset expectation maximization with the use of a postreconstruction Gaussian filter (5-mm full width half maximum).

PET/CT images were interpreted in standard clinical fashion, both separately and in a fused mode. PET/CT images were reviewed for abnormal FDG uptake at the primary tumor site, lymph node regions, and distant sites. The three-dimensional volume of the primary tumor was calculated and recorded using the 40% threshold method, as described previously (20). Briefly, this method identifies tumor as any voxel in the three-dimensional data set with counts greater than a fixed threshold fraction of the peak activity in the tumor. The 40% threshold level was determined by optimized correlation with the CT dimensions of the primary tumor. A posttherapy FDG-PET/CT was done 3 mo after completing radiation treatment to evaluate response and any residual or progressive disease (21, 22).

Heterogeneity evaluation. From each patient's FDG-PET/CT study, a threshold-volume curve (Fig. 1A) was generated. A region of interest was manually drawn to fully include the primary tumor and a surrounding region of normal tissue (normal background). FDG is excreted in the urine, and therefore, the urinary bladder activity was excluded from the region of interest. Image segmentation to determine the threshold values was done using an adaptive thresholding method to adjust for each patient's tumor and to account for variations in the image contrast and normal tissue background (23). This process used the Siemens e.soft software. An optimized exponential function was calculated to fit to the threshold-volume curve (Fig. 1A) by minimizing the residuals and calculating thresholds from 0 to 100%, similar to the method of Erdi et al. (24). The fitted curves (one for each patient) took the form of the following general equation:

$$T = T_O e^{-\lambda V} \quad (A)$$

wherein T is specific segmented threshold value, T_O is threshold of the smallest segmented volume, λ is volume rate constant, and V is tumor volume (cubic centimeters).

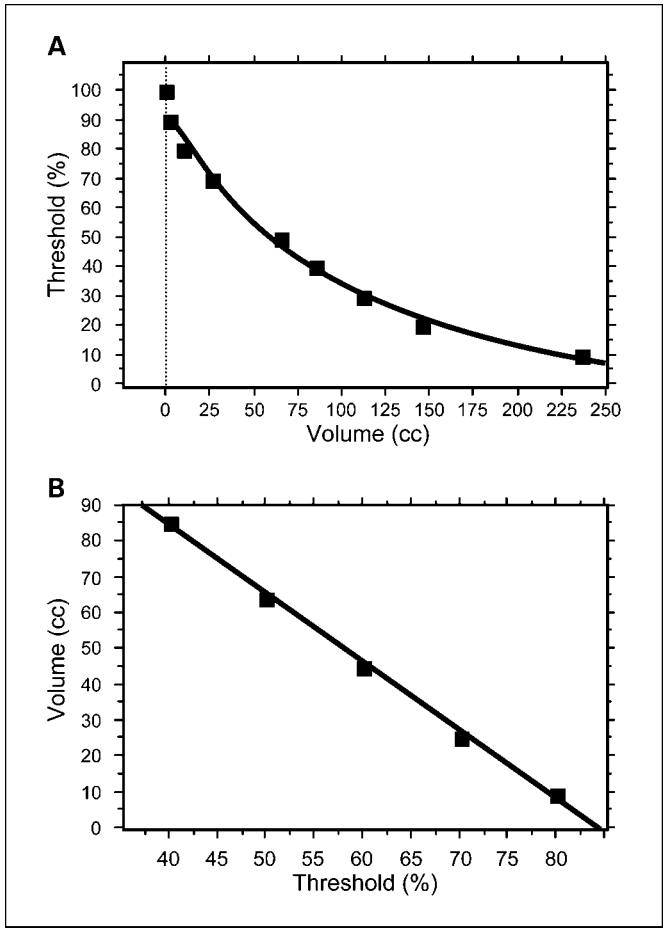

Fig. 1. *A,* the threshold-volume curve compares the threshold (%) to the volume segmented by that threshold. A threshold-volume curve is derived for each patient. *B,* the volume-threshold function from which intratumoral heterogeneity, H (dV/dT), is derived. These data are for the patient shown in *A*.

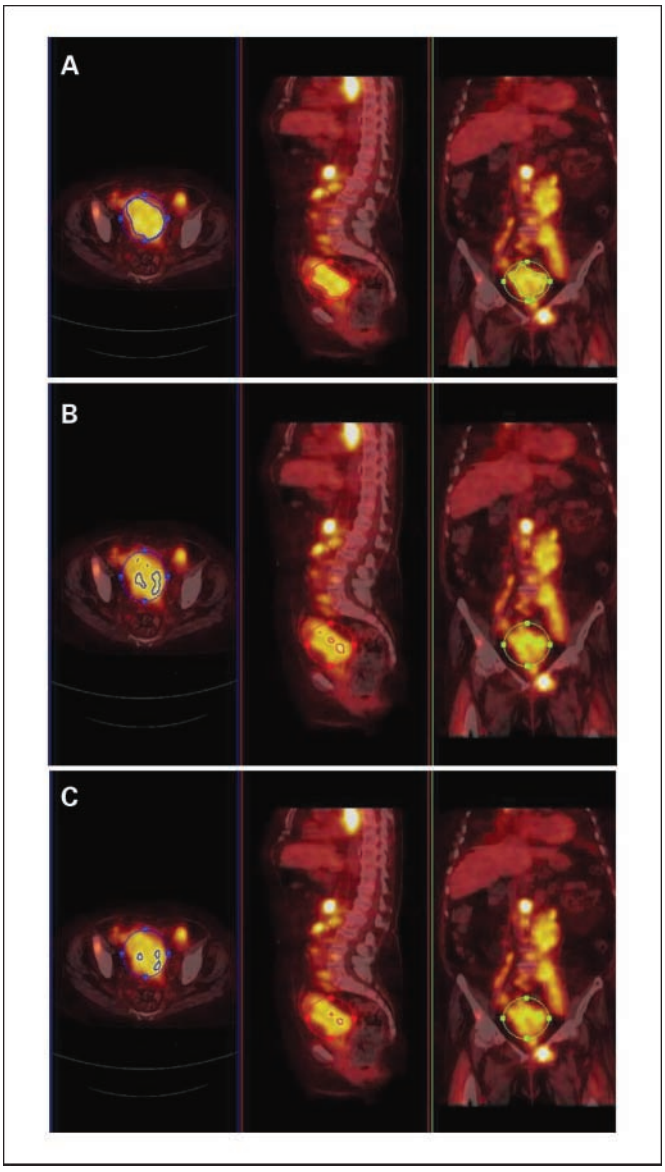

Fig. 2. A region of interest is drawn around the primary cervix tumor and the surrounding normal tissue. *A*, the 40% threshold represents the "actual" tumor volume. Decreasing volumes are represented by the 60% threshold (*B*) and the 80% threshold (*C*). From left to right, images are shown in axial, sagittal, and coronal planes.

To determine tumor heterogeneity, we next plotted tumor volume (V) resulting from the previously defined threshold values (T) as calculated in Eq. (A) (Fig. 1B). Our previous work showed that the minimal threshold that represents the actual tumor volume for cervical cancer was 40%; therefore, all values of <40% were eliminated from the heterogeneity analysis (values of <40% represent normal tissue background activity and not tumor). In addition, all values of >80% were eliminated because the volumes were small and the partial volume effect was pronounced (25). Typically, these volumes were <5 cm^3. The linear regression curves (one for each patient) took the form of the following general equation:

$$V = G - HT \quad \text{(B)}$$

wherein V is tumor volume (cm^3), G is constant, T is threshold (%), H (dV/dT) is heterogeneity.

Heterogeneity is therefore represented by the slope of the regression line in Fig. 1B. The increased steepness of this slope is indicative of increasing variability of glucose metabolism across the entirety of the volume of the tumor. Heterogeneity is therefore independent of the absolute volume and absolute value of the glucose uptake. Figure 2 shows the initial region of interest consisting of tumor and background normal tissue. The 40%, 60%, and 80% thresholds are shown. It is important to note that the %T volumes may not be contiguous throughout the entire volume of the tumor and that "islands" of increased glucose metabolism may occur.

In summary, the thresholds are firstly determined from a volume that includes both tumor and normal background tissue. Then, normal background tissue (T < 40%) was excluded. T > 80% was excluded because these values represent very small volumes (typically <5 cm^3). H is then calculated from %T versus V regression line.

Outcome evaluation. Sites of lymph node involvement were evaluated on the initial diagnostic FDG-PET/CT. Patients had follow-up physical examinations approximately every 2 mo for the first 6 mo, every 3 mo for the next 2 y, and then every 6 mo. The FDG-PET/CT was repeated 3 mo after completion of treatment and then yearly or when warranted by clinical examination or symptoms. Disease status, including pelvic recurrences, distant metastatic disease, and death were recorded.

Statistical Analysis. Clinical-pathologic factors and outcome data were analyzed for correlation with tumor heterogeneity. Survival and tumor recurrence were measured from the completion of treatment. StatView, SAS Institute, Inc. Version 5.0.1 software was used for the analysis. P < 0.05 was set as the threshold for significance for all study outcomes. The Kaplan-Meier (product limit) method was used to derive estimates of survival based on total sample size (26). Tests of equivalence of estimates of survival and stratification into high and low heterogeneity groups were done by the generalized Wilcoxon log-rank test (27). Mann-Whitney nonparametric analysis (28) was used to evaluate the correlation between tumor heterogeneity on pretreatment FDG-PET and tumor histology, risk of lymph node metastasis at diagnosis, treatment response, and risk of pelvic recurrence.

Multivariate analysis was done using the Cox proportional hazards regression model to evaluate the effect of tumor heterogeneity and other risk factors on pelvic recurrence (29). The Cox model used to evaluate pelvic recurrence outcome was done as a stepwise procedure using a P-to-enter value and a P-to-remove value of 0.05. The assumption of proportionality was tested and met. The time-dependent outcome variable that was tested was pelvic recurrence. Variables initially tested in the model included tumor and treatment-related factors believed to be of significance in this population of patients with advanced stage cervical cancer. The variables entered into the first model were clinical stage, pretreatment lymph node status, total radiation treatment time, and number of cycles of chemotherapy as predictors of pelvic recurrence. The forward stepwise procedure using a P-to-enter value and a P-to-remove value of 0.05 failed to allow total radiation treatment time and number of cycles of chemotherapy into the model (data not shown).

The next multivariate proportional hazards model was constructed using the remaining variables of clinical stage and pretreatment lymph node status. The variables of tumor volume, SUV_{Max}, and heterogeneity were added to this second model. The forward stepwise procedure using a P-to-enter value and a P-to-remove value of 0.05 failed to allow clinical stage and pretreatment lymph node status to remain in the model. The final model that was constructed consisted of the variables: SUV_{Max}, heterogeneity, and tumor volume.

Logistic modeling was also done to evaluate the three variables of SUV_{Max}, heterogeneity, and tumor volume on the end point: posttherapy FDG-PET status as described in our previous paper (22).

Results

Patients characteristics and tumor status

Patient characteristics, including age at diagnosis, International Federation of Gynecology and Obstetrics clinical stage, histology, and lymph node status at diagnosis, are listed in Table 1. The mean SUV_{Max} was 12.4 (range, 3.0-38.4). The mean tumor volume was 47.6 cm^3 (range, 4.8-264.2 cm^3).

At the time of last follow-up, 27 patients had developed recurrent disease, 45 were free of disease, 12 died from progressive disease, and 60 patients were alive (15 were alive with disease present). The sites of recurrence were pelvic recurrence only in 6 patients, distant metastases only in 11 patients, and 10 patients developed both a pelvic recurrence and distant metastases.

Tumor heterogeneity

Tumor-specific factors. Intratumoral heterogeneity, H, as measured by dV/dT from the regression analysis, showed a mean heterogeneity of -1.074 (range, -0.107 to -5.623). This represents a 50-fold intertumoral change in heterogeneity. A scattergram of these values, arranged according to clinical tumor stage, is shown in Fig. 3A. This shows the variability in heterogeneity among tumors of the same International Federation of Gynecology and Obstetrics clinical stage. The relationships between intratumoral heterogeneity and other tumor specific factors were evaluated. There was no significant association between tumor heterogeneity and SUV_{Max} of the primary tumor ($R^2 = 0.069$). This is shown in Fig. 3B. The effect of the primary tumor volume on heterogeneity was also evaluated (Fig. 3C). There was a trend for larger tumors to be more heterogeneous ($R^2 = 0.881$). There was no association between intratumoral heterogeneity and tumor histologic subtype ($P = 0.4905$). The relationship between lymph node status at diagnosis and cervical tumor heterogeneity was analyzed and showed that greater heterogeneity was associated with an increased likelihood of lymph node metastasis ($P = 0.0009$).

Tumor response and survival. The mean follow-up for all patients alive and free of disease at the time of last follow-up was 21.1 months (range, 7-61 months). Patients underwent an FDG-PET 3 months after completing chemoradiation to assess their metabolic response to treatment. Mann-Whitney analysis showed that tumor heterogeneity was significantly associated with tumor response to radiation ($P = 0.0207$), with greater heterogeneity being associated with increased risk of an incomplete metabolic response on the 3-month posttreatment FDG-PET/CT. Tumor heterogeneity was also significantly associated with the risk of tumor recurrence in the pelvis ($P = 0.0017$) and progression-free survival ($P = 0.03$; Fig. 4).

Cox proportional hazards modeling for pelvic recurrence showed that tumor volume, as determined by FDG-PET, was the most significant predictive factor of pelvic recurrence ($P = 0.0003$) with a hazard ratio of 1.015 (95% confidence interval, 0.999-1.033; Table 2). Tumor heterogeneity was the next most significant predictive factor of pelvic recurrence ($P = 0.0035$) with a hazard ratio of 1.074 (95% confidence interval, 0.476-2.422). SUV_{Max} did not remain a significant predictor ($P = 0.5713$) in this model. The logistic model using the posttherapy FDG-PET as the time-independent end point showed FDG-PET tumor volume ($P = 0.0110$) and heterogeneity ($P = 0.0325$) as significant predictive factors for a positive posttherapy FDG-PET, but SUV_{Max} was not predictive ($P = 0.3755$).

Discussion

We hypothesized that intratumoral metabolic heterogeneity of primary cervix tumors could be quantified and may be of prognostic significance. We found that FDG uptake varies across tumors, and this intratumoral heterogeneity is not significantly related to tumor stage, tumor histology, or primary tumor SUV_{Max}. Nevertheless, it has some association to tumor volume. We found that cervical intratumor heterogeneity, as

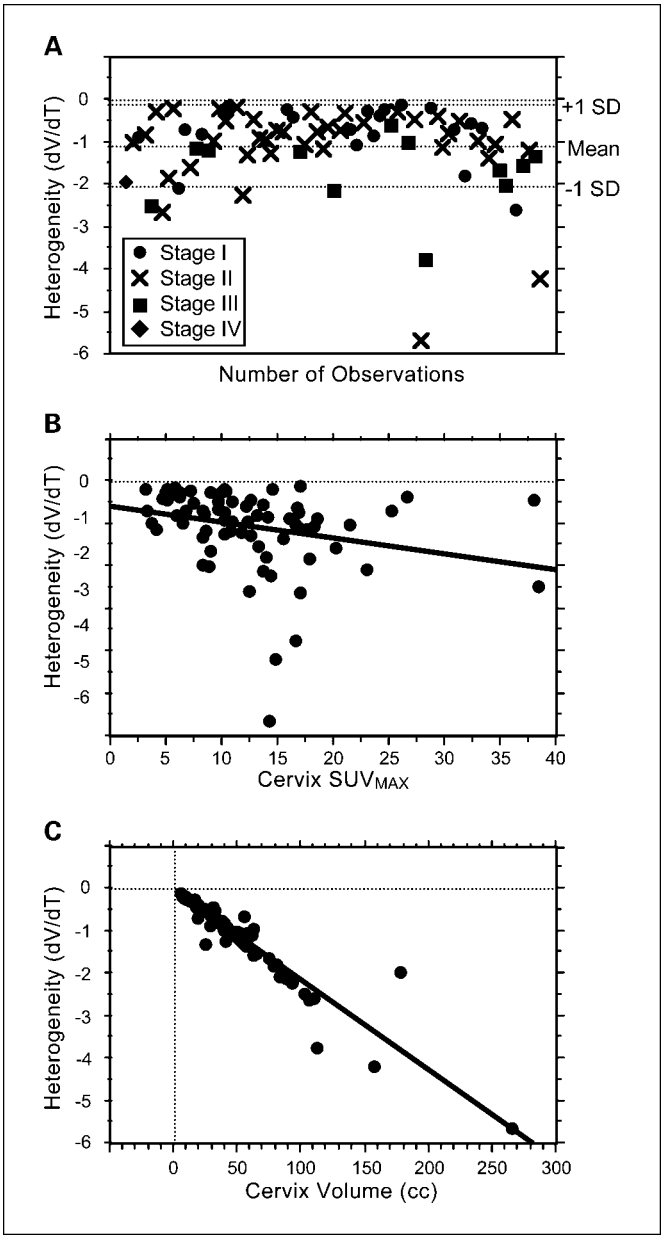

Fig. 3. *A,* scattergram of intratumoral heterogeneity in the patient population by International Federation of Gynecology and Obstetrics clinical tumor stage. *B,* relationship of intratumoral heterogeneity and tumor SUV_{Max}. *C,* relationship of intratumoral heterogeneity and tumor volume.

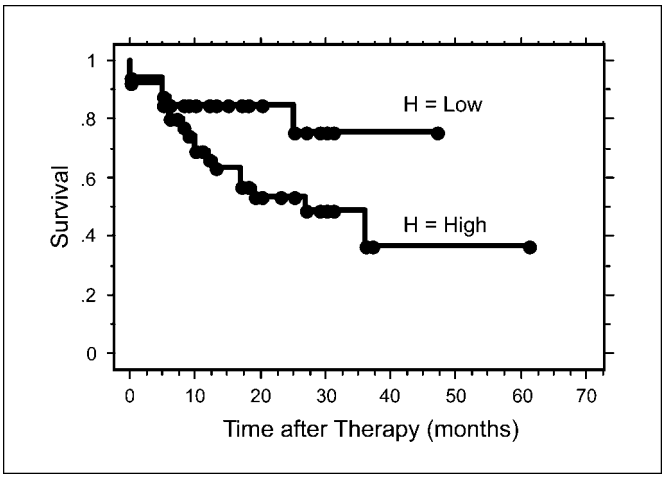

Fig. 4. Progression-free survival comparing patients with low versus high heterogeneity tumors. $P = 0.03$.

seen on pretreatment FDG-PET, predicts the risk of lymph node involvement at diagnosis, treatment response to radiation, risk of pelvic recurrence, and progression-free survival. Our group and others have shown the prognostic value of SUV_{Max}. In particular, higher SUV_{Max} levels predict a worse outcome (16, 17, 30, 31). Our current work shows that intratumoral metabolic heterogeneity is a distinct predictive tool with no significant association with SUV_{Max}. Additionally, with Cox multivariate analysis, the risk of pelvic recurrence was better predicted by heterogeneity than by SUV_{Max}.

Cervical tumor response during therapy (32) and the absence of abnormal FDG uptake on the posttherapy PET (21, 22) are predictive of survival outcome. The current study found that high primary intratumoral heterogeneity at diagnosis was predictive of subsequent pelvic recurrence and was correlated with persistent tumor on the posttherapy PET image. Other researchers have found that lack of cervical tumor regression during therapy, as evaluated by physical examination, CT, and magnetic resonance spectroscopy, are associated with an inferior outcome (33–36). Achieving local control is critical to prognosis and overall survival, and having a biomarker at diagnosis predictive of treatment response could be very valuable.

This work is significant because it provides a novel, yet readily available, prognostic tool quantifying and relating intratumoral heterogeneity on FDG-PET at diagnosis to outcome measures. Some studies have shown the variation in tumor microenvironments with small changes in local heterogeneity. Other groups have shown intertumoral heterogeneity of FDG uptake for tumors (7, 9, 37). However, only a few studies have been published evaluating the clinical significance of intratumoral heterogeneity and outcome measures. For head and neck cancer and non–small cell lung cancer, some preliminary data suggests radiation treatment outcome can be associated with kinetic behavior of 18F-MISO PET (38). O'Sullivan and colleagues noticed that FDG heterogeneity of malignant sarcoma was associated with time to patient death (37, 39).

We have shown that cervical tumors show metabolic heterogeneity on FDG-PET and that this heterogeneity correlates with various outcome measures, but the specific cause for this heterogeneity remains somewhat uncertain. Brown and colleagues found a relationship between FDG uptake in human non–small cell lung cancers and GLUT-1 expression by immunohistochemistry (40). Mayer and associates were unable to show a positive relationship between GLUT-1 expression by immunohistochemistry and hypoxia in patients with advanced cervical cancer (41). Other groups have suggested that FDG uptake may be correlated with hypoxia, cellular proliferation, and blood flow (7). For head and neck cancers, it has been shown that high lactate levels correlate with worse survival, increased risk of metastasis (42), and radiosensitivity (43).

A possible limitation of our study may be the association of the intratumoral heterogeneity to tumor volume. It could be that a larger-volume tumor provides a greater opportunity for heterogeneity, or it could be that greater heterogeneity leads to larger tumors. Modeling studies have shown that under low tissue oxygen concentrations and anaerobic glycolysis, tumors develop more aggressive phenotypes with low apoptotic potential, which can lead to larger tumors (44). Additionally, we noticed that some large-volume tumors showed a small amount of heterogeneity, whereas some smaller tumors showed significant heterogeneity. Clinical stage of disease is related to tumor volume; that is, tumor volumes tend to be greater for higher clinical stages of disease. Figure 3A is a scattergram of tumor heterogeneity that shows the variability of heterogeneity and clinical stage. In addition, one key feature of tumor heterogeneity is shown in Fig. 2. These images show that increasing the thresholding level decreases the contoured volume and that these volumes are not contiguous (i.e., there are insular regions of high glucose metabolism). This noncontinuity is not taken into account in our current heterogeneity model, but we are developing a methodology to evaluate this property.

In analyzing radiation dose, tumor volume, and tumor control probability, Bentzen and Thames conclude that, "because of heterogeneity in patient and tumor characteristics,

Table 2. Cox proportional-hazards modeling parameters for pelvic recurrence

	FDG-PET tumor volume	Heterogeneity	SUV_{Max}
Coefficient	0.015	0.071	0.011
SE	0.008	0.415	0.043
Coefficient/SE	1.810	0.171	0.246
X^2	12.965	8.540	0.321
Hazard ratio (95% confidence interval)	1.015 (0.999-1.033)	1.074 (0.476-2.422)	1.011 (0.929-1.099)
P	0.0003	0.0035	0.5713

the volume effect is less pronounced than would be expected from a simple proportionality between number of clonogens and volume." Our previously published clinical data supports this hypothesis. We have shown a radiation-dose-response relationship for patients with cervical cancer by tumor stage and that pelvic tumor cure plateaus at ~85 Gy irrespective of tumor stage (45). It seems that intratumoral heterogeneity provides additional information beyond volume, which helps clarify tumor behavior.

The next steps to investigating tumor heterogeneity as a prognostic factor include validating this metric on a new group of patients, developing other metrics for measuring gross tumor FDG heterogeneity, and further investigating the biological mechanism causing this cervical tumor heterogeneity on FDG-PET. This may lead to prospectively targeting patients with high heterogeneity cervical tumors with more aggressive therapy.

Disclosure of Potential Conflicts of Interest

No potential conflicts of interest were disclosed.

References

1. Thomlinson RH, Gray LH. The Histological Structure of Some Human Lung Cancers and the Possible Implications for Radiotherapy. Br J Cancer 1955;9:539–49.
2. Heppner GH. Tumor heterogeneity. Cancer Res 1984; 44:2259–65.
3. Alexandrova R. Tumour heterogeneity. Exp Pathol Parasitol 2001;6:57–67.
4. Britten RA, Evans AJ, Allalunis-Turner MJ, Franko AJ, Pearcey RG. Intratumoral heterogeneity as a confounding factor in clonogenic assays for tumour radioresponsiveness. Radiother Oncol 1996;39:145–53.
5. Hockel M, Schlenger K, Aral B, Mitze M, Schaffer U, Vaupel P. Association between tumor hypoxia and malignant progression in advanced cancer of the uterine cervix. Cancer Res 1996;56:4509–15.
6. Delorme S, Knopp MV. Non-invasive vascular imaging: assessing tumour vascularity. Eur Radiol 1998;8:517–27.
7. Pugachev A, Ruan S, Carlin S, et al. Dependence of FDG uptake on tumor microenvironment. Int J Radiat Oncol Biol Phys 2005;62:545–53.
8. Thorwarth D, Eschmann SM, Paulsen F, Alber M. A model of reoxygenation dynamics of head-and-neck tumors based on serial 18F-fluoromisonidazole positron emission tomography investigations. Int J Radiat Oncol Biol Phys 2007;68:515–21.
9. Zhao S, Kuge Y, Mochizuki T, et al. Biologic correlates of intratumoral heterogeneity in 18F-FDG distribution with regional expression of glucose transporters and hexokinase-II in experimental tumor. J Nucl Med 2005;46:675–82.
10. Bachtiary B, Boutros PC, Pintilie M, et al. Gene expression profiling in cervical cancer: an exploration of intratumor heterogeneity. Clin Cancer Res 2006;12: 5632–40.
11. Schwarz JK, Rader JS, Huettner PC, Watson MA, Grigsby PW. Molecular Characterization of FDG-PET Metabolic Response in Cervical Cancer. Int J Radiat Oncol Biol Phys 2007;69:S115.
12. Davidson SE, West CM, Roberts SA, Hendry JH, Hunter RD. Radiosensitivity testing of primary cervical carcinoma: evaluation of intra- and inter-tumour heterogeneity. Radiother Oncol 1990;18:349–56.
13. Grigsby PW, Watson M, Powell MA, Zhang Z, Rader JS. Gene expression patterns in advanced human cervical cancer. Int J Gynecol Cancer 2006;16:562–7.
14. Dehdashti F, Grigsby PW, Mintun MA, Lewis JS, Siegel BA, Welch MJ. Assessing tumor hypoxia in cervical cancer by positron emission tomography with 60Cu-ATSM: relationship to therapeutic response-a preliminary report. Int J Radiat Oncol Biol Phys 2003; 55:1233–8.
15. Dehdashti F, Grigsby PW, Lewis JS, Laforest R, Siegel BA, Welch MJ. Assessing tumor hypoxia in cervical cancer by PET with 60 Cu-labeled diacetyl-bis(*N*4-methylthiosemicarbazone). J Nucl Med 2008;49:201–5.
16. Xue F, Lin LL, Dehdashti F, Miller TR, Siegel BA, Grigsby PW. F-18 fluorodeoxyglucose uptake in primary cervical cancer as an indicator of prognosis after radiation therapy. Gynecol Oncol 2006;101:147–51.
17. Kidd EA, Siegel BA, Dehdashti F, Grigsby PW. The standardized uptake value for F-18 fluorodeoxyglucose is a sensitive predictive biomarker for cervical cancer treatment response and survival. Cancer 2007;110:1738–44.
18. Miller TR, Pinkus E, Dehdashti F. Improved prognostic value of 18F-FDG PET using a simple visual analysis of tumor characteristics in patients with cervical cancer. J Nucl Med 2003;44:192–7.
19. MacDonald D, Lin L, Wahab S, et al. Combined IMRT and brachytherapy in the treatment of intact cervical cancer. Int J Radiat Oncol Biol Phys 2006;66: S43.
20. Miller TR, Grigsby PW. Measurement of tumor volume by PET to evaluate prognosis in patients with advanced cervical cancer treated by radiation therapy. Int J Radiat Oncol Biol Phys 2002;53:353–9.
21. Grigsby PW, Siegel BA, Dehdashti F, Rader J, Zoberi I. Posttherapy [^{18}F] fluorodeoxyglucose positron emission tomography in carcinoma of the cervix: response and outcome. J Clin Oncol 2004;22: 2167–71.
22. Schwarz JK, Siegel BA, Dehdashti F, Grigsby PW. Association of posttherapy positron emission tomography with tumor response and survival in cervical carcinoma. JAMA 2007;298:2289–95.
23. Long DT, King MA, Sheehan J. Comparative evaluation of image segmentation methods for volume quantitation in SPECT. Med Phys 1992;19:483–9.
24. Erdi YE, Wessels BW, Loew MH, Erdi AK. Threshold estimation in single photon emission computed tomography and planar imaging for clinical radioimmunotherapy. Cancer Res 1995;55:5823–6s.
25. Soret M, Bacharach SL, Buvat I. Partial-volume effect in PET tumor imaging. J Nucl Med 2007;48: 932–45.
26. Kaplan EL, Meier P. Nonparametric estimation from incomplete observations. JAMA 1958;53:457–81.
27. Breslow N. A generalized Kruskal-Wallis test for comparing K samples subject to unequal patterns of censorship. Biometrika 1970;57:579–94.
28. Mann HB, Whitney DR. On a test of whether one of two random variables is stochastically larger than the other. Ann Math Stat 1947;18:50–60.
29. Cox DR. Regression models and life tables. JSTOR 1972;34:187–220.
30. Pillot G, Siegel BA, Govindan R. Prognostic significance of fluorodeoxyglucose positron emission tomography in non-small cell lung cancer: a review. J Thorac Oncol 2006;1:152–9.
31. Schwartz DL, Rajendran J, Yueh B, et al. FDG-PET prediction of head and neck squamous cell cancer outcomes. Arch Otolaryngol Head Neck Surg 2004; 130:1361–7.
32. Lin LL, Yang Z, Mutic S, Miller TR, Grigsby PW. FDG-PET imaging for the assessment of physiologic volume response during radiotherapy in cervix cancer. Int J Radiat Oncol Biol Phys 2006;65:177–81.
33. Hardt N, van Nagell JR, Hanson M, Donaldson E, Yoneda J, Maruyama Y. Radiation-induced tumor regression as a prognostic factor in patients with invasive cervical cancer. Cancer 1982;49:35–9.
34. Hong JH, Chen MS, Lin FJ, Tang SG. Prognostic assessment of tumor regression after external irradiation for cervical cancer. Int J Radiat Oncol Biol Phys 1992;22:913–7.
35. Lee CM, Shrieve DC, Gaffney DK. Rapid involution and mobility of carcinoma of the cervix. Int J Radiat Oncol Biol Phys 2004;58:625–30.
36. Potter R, Dimopoulos J, Georg P, et al. Clinical impact of MRI assisted dose volume adaptation and dose escalation in brachytherapy of locally advanced cervix cancer. Radiother Oncol 2007;83:148–55.
37. O'Sullivan F, Roy S, Eary J. A statistical measure of tissue heterogeneity with application to 3D PET sarcoma data. Biostatistics 2003;4:433–48.
38. Eschmann SM, Friedel G, Paulsen F, et al. Is standardised (18) F-FDG uptake value an outcome predictor in patients with stage III non-small cell lung cancer? Eur J Nucl Med Mol Imaging 2006;33:263–9.
39. O'Sullivan F, Roy S, O'Sullivan J, Vernon C, Eary J. Incorporation of tumor shape into an assessment of spatial heterogeneity for human sarcomas imaged with FDG-PET. Biostatistics 2005;6:293–301.
40. Brown RS, Leung JY, Kison PV, Zasadny KR, Flint A, Wahl RL. Glucose transporters and FDG uptake in untreated primary human non-small cell lung cancer. J Nucl Med 1999;40:556–65.
41. Mayer A, Hockel M, Wree A, Vaupel P. Microregional expression of glucose transporter-1 and oxygenation status: lack of correlation in locally advanced cervical cancers. Clin Cancer Res 2005;11:2768–73.
42. Brizel DM, Schroeder T, Scher RL, et al. Elevated tumor lactate concentrations predict for an increased risk of metastases in head-and-neck cancer. Int J Radiat Oncol Biol Phys 2001;51:349–53.
43. Quennet V, Yaromina A, Zips D, et al. Tumor lactate content predicts for response to fractionated irradiation of human squamous cell carcinomas in nude mice. Radiother Oncol 2006;81:130–5.
44. Gerlee P, Anderson AR. An evolutionary hybrid cellular automaton model of solid tumour growth. J Theor Biol 2007;246:583–603.
45. Perez CA, Grigsby PW, Chao KS, Mutch DG, Lockett MA. Tumor size, irradiation dose, and long-term outcome of carcinoma of uterine cervix. Int J Radiat Oncol Biol Phys 1998;41:307–17.